Biological Forum – An International Journal **15(5a): 757-766(2023)**

ISSN No. (Print): 0975-1130
ISSN No. (Online): 2249-3239

Synthesis and Antimicrobial Activity of imidazo [4,5-b] indole Derivatives

Bhumika Ranawat[1*], Renu Rathore[1], Ritu Tomar[1] and Mangal Shree Dulawat[2]
[1]Bhupal Nobles' University, Udaipur (Rajasthan), India.
[2]Janardan Rai Nagar Rajasthan Vidhyapeeth (Deemed-to-be) University Udaipur (Rajasthan), India.

(Corresponding author: Bhumika Ranawat)*
(Received: 03 April 2023; Revised: 22 April 2023; Accepted: 07 May 2023; Published: 15 May 2023)
(Published by Research Trend)

ABSTRACT: A series of imidazo[4,5-*b*] indole derivatives 3(a-o) were synthesized. The *in vitro* antimalarial activity of the synthesized compounds against different antimicrobial strains was assessed. Both *in silico* ADMET prediction and molecular docking investigations were conducted. The two most potent compounds in the series were identified 3i, and 3k with respective values of *E. coli* Dihydrorootase complex and GyrB of *S. aureus*. At the binding site, molecular dynamics simulations were run on the most active molecules, 3c, and 3h for 2EG7 PDB, and3e, and 3g for 5D6P PDB.

Keywords: Synthesis, antimicrobial activity, imidazo[4,5-b]indole, molecular docking.

INTRODUCTION

Currently, numerous communities are impacted by cancer. In 2012, there were 14.2 million newly diagnosed cases of cancer and 8.2 million deaths attributed to the disease. It is projected that by 2030, the number of new cancer cases will rise to approximately 19 million (Russo *et al*., 2015; Torre *et al*., 2015).

Antimicrobial Resistance (AMR) refers to the ability of microorganisms, such as bacteria, viruses, fungi, and parasites, to adapt and thrive in the presence of drugs that previously affected them. Antimicrobial resistance (AMR) poses a substantial risk to public health systems, not only in underdeveloped nations but globally (Abushaheen *et al*., 2020; Barman *et al*., 2023; Ferri *et al*., 2017; Kumar & Nanda 2021; Malaviya & Mishra 2011; Marston *et al*., 2016). The emergence of antibiotic-resistant infectious illnesses heralds an uncertain future in the field of healthcare. Contracting antimicrobial resistance (AMR) results in severe ailments and extended stays in medical facilities, as well as elevated expenses in healthcare, increased expenditures in alternative medications, and instances of treatment ineffectiveness (De Villiers, 2019; Ziegler, 2014). For example, in Europe alone, it has been projected that antibiotic resistance is associated with an economic burden of over nine billion euros annually. Moreover, as stated by the Centers for Disease Control and Prevention (CDC), antibiotic resistance results in an additional $20 billion in direct healthcare expenses in the United States, not including an estimated $35 billion in annual productivity losses (Hillock *et al*., 2022; Peyrani *et al*., 2019; Hashiguchi *et al*., 2019).

The formidable menace of antimicrobial resistance is especially significant in the realm of antibiotic resistance in bacteria. As per the CDC, about two million individuals in the United States contract antibiotic-resistant infections annually, leading to a minimum of 23,000 fatalities. Antibiotic resistance weakens the ability of a human immune system to combat infectious infections and also leads to various difficulties in susceptible patients undergoing chemotherapy, dialysis, surgery, and joint replacement. In addition, individuals suffering from chronic ailments such as diabetes, asthma, and rheumatoid arthritis would experience significant consequences as a result of antibiotic resistance. Given the ongoing persistence of antimicrobial resistance (AMR), it is advisable for physicians to resort to last-resort classes of medicine, such as carbapenems and polymyxins. However, it is important to note that these medications may not be easily accessible in developing countries, are expensive, and can cause various side effects (Ballal, 2016; Duvvi *et al.,* 2019; Kaur *et al.,* 2019; Makena *et al*., 2016; Marshall *et al*., 2014; Sharma, 2010; Waithaka*et al*., 2017).

In this work, we describe a medicinal chemistry strategy consisting of the design, synthetic preparation and antimicrobial evaluation of a series of imidazo[4,5-*b*]indole derivatives.

MATERIAL AND METHOD

Chemistry. All the melting points reported were determined by open capillary tube method and are uncorrected. The synthesis and analytical studies of the compounds were carried out using laboratory grade and analytical grade reagents as the case may be a standard procedure or reported method was followed with or without modificationappropriately as and when required. Elemental analysis (C, H, and N) was undertaken with a Perkin-Elmer model 240C analyzer, and all analyses were consistent with theoretical values (within 0.4%) unless indicated. IR absorption spectra were recorded on Bruker alpha. ^{1}H NMR spectra were recorded on the Bruker DPX-400 instrument at 400 MHz. The ^{1}H chemical shifts are reported as parts per

million (ppm) downfield from TMS (Me4Si). The LC mass spectra of the compounds were recorded on the Shimadzu 8201PC spectrometer. The homogeneity of the compounds was monitored by ascending thin-layer chromatography (TLC) on silica gel G (Merck)-coated aluminum plates, visualized by iodine vapor.

7-methoxy-4-methyl-2-(o-tolyl)-3,3a,4,8b-tetrahydroimidazo[4,5-b]indole (3a). Melting Point: 216-220ºC.Yield: 86 %.R_f value: 0.72.Solvent system: Benzene: Methanol (9.7: 0.3). Anal. Calcd. for $C_{18}H_{19}N_3O$ (293.36): C, 73.69; H, 6.53; N, 14.32, Found: C, 73.59; H, 6.43; N, 14.12.IR (υ_{max}, cm^{-1}): 3424 (N-H), 3044 (Ar. C–H), 2927 (C–H aliphatic), 1542 (C=N), 1467 (Ar. C=C), 1163 (C–N), 1054 (C-O).^{1}H NMR (400 MHz, $CDCl_3$); δ: 7.57 (dd, *J* = 1.7 Hz, 1H), 7.28 – 7.24 (m, 1H), 7.21 – 7.17 (m, 2H), 6.58 (s, 2H), 6.53 (s, 1H), 5.51 (d, *J* = 7.0 Hz, 1H), 4.38 (d, *J* = 7.3 Hz, 1H), 3.82 (s, 3H), 2.91 (s, 3H), 2.37 (s, 3H), 1.68 (s, 1H).LCMS: Calculated for $C_{18}H_{19}N_3O$ $[M+H]^+$293.36, found 293.40.

7-methoxy-4-methyl-2-(p-tolyl)-3,3a,4,8b-tetrahydroimidazo[4,5-b]indole (3b). Melting Point: 222-226ºC. Yield: 82 %.R_f value: 0.72.Solvent system: Benzene: Methanol (9.7: 0.3). Anal. Calcd. for $C_{18}H_{19}N_3O$ (293.36): C, 73.69; H, 6.53; N, 14.32, Found: C, 73.49; H, 6.23; N, 14.12.IR (υ_{max}, cm^{-1}): 3458 (N-H), 3015 (Ar. C–H), 2953 (C–H aliphatic), 1525 (C=N), 1447 (Ar. C=C), 1135 (C–N), 1067 (C-O).^{1}H NMR (400 MHz, $CDCl_3$); δ: 7.54 (d, *J*= 7.0Hz, 2H), 7.19 (d, *J* = 7.2Hz, 2H), 6.59 (s, 1H), 6.57 (s, 2H), 5.84 (d, *J* = 7.3 Hz, 1H), 4.38 (d, *J* = 7.1 Hz, 1H), 3.81 (s, 3H), 2.91 (s, 3H), 2.35 (s, 3H), 1.92 (s, 1H). LCMS: Calculated for $C_{18}H_{19}N_3O$ $[M+H]^+$293.36, found 293.39.

2-(2,6-dimethylphenyl)-7-methoxy-4-methyl-3,3a,4,8b-tetrahydroimidazo[4,5-b]indole (3c). Melting Point: 200-204ºC.Yield: 84 %. R_f value: 0.59. Solvent system: Benzene: Methanol (9.7: 0.3). Anal. Calcd. for $C_{19}H_{21}N_3O$ (307.39): C, 74.24; H, 6.89; N, 13.67, Found: C, 74.04; H, 6.69; N, 13.47.IR (υ_{max}, cm^{-1}): 3482 (N-H), 3047 (Ar. C–H), 2968 (C–H aliphatic), 1534 (C=N), 1486 (Ar. C=C), 1174 (C–N), 1024 (C-O).^{1}H NMR (400 MHz, $CDCl_3$); δ: 7.23 (dd,*J* = 1.5Hz, 1H), 7.08 (d, *J* = 7.2Hz, 2H), 6.65 – 6.57 (m, 3H), 5.36 (d, *J* = 7.3 Hz, 1H), 4.38 (d, *J* = 7.1 Hz, 1H), 3.81 (s, 3H), 2.91 (s, 3H), 2.36 (s, 3H), 1.66 (s, 1H).LCMS: Calculated for $C_{19}H_{21}N_3O$ $[M+H]^+$307.39, found 307.42.

2-(2-fluorophenyl)-7-methoxy-4-methyl-3,3a,4,8b-tetrahydroimidazo[4,5-b]indole (3d). Melting Point: 188-192ºC.Yield: 84 %.R_f value: 0.64.Solvent system: Benzene: Methanol (9.7: 0.3). Anal. Calcd. for $C_{17}H_{16}FN_3O$ (297.33): C, 68.67; H, 5.42; N, 14.13. Found: C, 68.57; H, 5.22; N, 14.03.IR (υ_{max}, cm^{-1}): 3398 (N-H), 3087 (Ar. C–H), 2968 (C–H aliphatic), 1539 (C=N), 1485 (Ar. C=C), 1198 (C–N), 1048 (C-O), 1025 (C-F).^{1}H NMR (400 MHz, $CDCl_3$); δ: 7.51 – 7.48 (m, 1H), 7.32 – 7.27 (m, 1H), 7.10 – 7.03 (m, 2H), 6.60 – 6.55 (m, 3H), 5.46 (d, *J* = 7.3 Hz, 1H), 4.38 (d, *J* = 7.1 Hz, 1H), 3.83 (s, 3H), 2.91 (s, 3H), 1.92 (s, 1H). LCMS: Calculated for $C_{17}H_{16}FN_3O$ $[M+H]^+$ 297.33, found 297.37.

7-methoxy-4-methyl-2-(4-(trifluoromethyl)phenyl)-3,3a,4,8b-tetrahydroimidazo[4,5-b]indole (3e) Melting Point: 212-216ºC.Yield: 81 %.R_f value: 0.62.Solvent system: Benzene: Methanol (9.7: 0.3). Anal. Calcd. for $C_{18}H_{16}F_3N_3O$ (347.33): C, 62.24; H, 4.64; N, 12.10.Found: C, 62.04; H, 4.44; N, 12.00.IR (υ_{max}, cm^{-1}): 3468 (N-H), 3088 (Ar. C–H), 2992 (C–H aliphatic), 1535 (C=N), 1475 (Ar. C=C), 1152 (C–N), 1014 (C-O), 1068 (C-F).^{1}H NMR (400 MHz, $CDCl_3$); δ: 7.60 – 7.55 (m, 4H), 6.63. – 6.54 (m, 3H), 5.52 (d, *J* = 7.3 Hz, 1H), 4.38 (d, *J* = 7.1 Hz, 1H), 3.81 (s, 3H), 2.90 (s, 3H), 1.88 (s, 1H).LCMS: Calculated for $C_{18}H_{16}F_3N_3O$ $[M+H]^+$347.33, found 347.36.

2-(2-chlorophenyl)-7-methoxy-4-methyl-3,3a,4,8b-tetrahydroimidazo[4,5-b]indole (3f). Melting Point: 218-222ºC.Yield: 79 %. R_f value: 0.66.Solvent system: Benzene: Methanol (9.7: 0.3). Anal. Calcd. for $C_{17}H_{16}ClN_3O$ (313.78): C, 65.07; H, 5.14; N, 13.39.Found: C, 65.07; H, 5.04; N, 13.29.IR (υ_{max}, cm^{-1}): 3488 (N-H), 3012 (Ar. C–H), 2957 (C–H aliphatic), 1542 (C=N), 1424 (Ar. C=C), 1163 (C–N), 1087 (C-O), 682 (C-Cl).^{1}H NMR (400 MHz, $CDCl_3$); δ: 7.60 (dd, *J* = 1.5 Hz, 1H), 7.34 (dd, *J* = 1.5 Hz, 1H), 7.27 – 7.18 (m, 2H), 6.60. – 6.53 (m, 3H), 5.58 (d, *J* = 7.3 Hz, 1H), 4.38 (d, *J* = 7.1 Hz, 1H), 3.83 (s, 3H), 2.92 (s, 3H), 2.47 (s, 1H).LCMS: Calculated for $C_{17}H_{16}ClN_3O$ $[M+H]^+$313.78, found 313.81.

2-(2,4-dichlorophenyl)-7-methoxy-4-methyl-3,3a,4,8b-tetrahydroimidazo[4,5-b]indole (3g). Melting Point: 228-232ºC.Yield: 77 %.R_f value: 0.65., Solvent system: Benzene: Methanol (9.7: 0.3). Anal. Calcd. for $C_{17}H_{15}Cl_2N_3O$ (348.23): C, 58.63; H, 4.34; N, 12.07. Found: C, 58.43; H, 4.24; N, 12.07.IR (υ_{max}, cm^{-1}): 3422 (N-H), 3064 (Ar. C–H), 2939 (C–H aliphatic), 1586 (C=N), 1415 (Ar. C=C), 1177 (C–N), 1040 (C-O), 715 (C-Cl).^{1}H NMR (400 MHz, $CDCl_3$);δ: 7.44 – 7.41 (m, 2H), 7.24 (dd, *J* = 1.5 Hz, 1H), 6.66 (d, *J* = 7.1 Hz, 1H), 7.61 – 6.56 (m, 2H), 5.31 (d, *J* = 7.3 Hz, 1H), 4.38 (d, *J* = 7.1 Hz, 1H), 3.85 (s, 3H), 2.90 (s, 3H), 1.86 (s, 1H).LCMS: Calculated for $C_{17}H_{15}Cl_2N_3O$ $[M+H]^+$348.23, found 348.23.

2-(2,6-difluorophenyl)-7-methoxy-4-methyl-3,3a,4,8b-tetrahydroimidazo[4,5-b]indole (3h). Melting Point: 204-208ºC. Yield: 76 %.R_f value: 0.68.Solvent system: Benzene: Methanol (9.7: 0.3). Anal. Calcd. for $C_{17}H_{15}F_2N_3O$ (288.39): C, 64.75; H, 4.79; N, 13.33.Found: C, 64.55; H, 4.69; N, 13.13.IR (υ_{max}, cm^{-1}): 3458 (N-H), 3042 (Ar. C–H), 2946 (C–H aliphatic), 1564 (C=N), 1484 (Ar. C=C), 1180 (C–N), 1071 (C-O), 1099 (C-F).^{1}H NMR (400 MHz, $CDCl_3$); δ: 7.31 – 7.27 (m, 1H), 6.84 (t, *J* = 6.7 Hz, 2H), 6.60 – 7.54 (m, 3H), 5.47 (d, *J* = 7.3 Hz, 1H), 4.38 (d, *J* = 7.1 Hz, 1H), 3.83 (s, 3H), 2.91 (s, 3H), 2.03 (s, 1H).LCMS: Calculated for $C_{17}H_{15}F_2N_3O$ $[M+H]^+$315.32, found 315.35.

2-(2-bromophenyl)-7-methoxy-4-methyl-3,3a,4,8b-tetrahydroimidazo[4,5-b]indole (3i). Melting Point: 226-230ºC.Yield: 81 %.R_f value: 0.72. Solvent system: Benzene: Methanol (9.7: 0.3). Anal. Calcd. for

$C_{17}H_{16}BrN_3O$ (358.23): C, 57.00; H, 4.50; N, 11.73. Found: C, 57.00; H, 4.40; N, 11.53.IR (υ_{max}, cm^{-1}): 3465 (N-H), 3018 (Ar. C–H), 2950 (C–H aliphatic), 1575 (C=N), 1426 (Ar. C=C), 1164 (C–N), 1035 (C-O), 528 (C-Br).^{1}H NMR (400 MHz, $CDCl_3$); δ: 7.58 (dd, *J* = 1.5 Hz, 1H), 7.50 (dd, *J* = 1.3 Hz, 1H), 7.28 – 7.17 (m, 2H), 6.62 – 7.56 (m, 3H), 5.65 (d, *J* = 7.3 Hz, 1H), 4.38 (d, *J* = 7.1 Hz, 1H), 3.83 (s, 3H), 2.92 (s, 3H), 2.46 (s, 1H). LCMS: Calculated for $C_{17}H_{16}BrN_3O$ $[M+H]^+$358.23, found 358.27.

7-methoxy-4-methyl-2-(4-(trifluoromethoxy)phenyl)-3,3a,4,8b-tetrahydroimidazo[4,5-b]indole (3j). Melting Point: 198-202ºC.Yield: 80 %.R_f value: 0.74. Solvent system: Benzene: Methanol (9.7: 0.3). Anal. Calcd. for $C_{18}H_{16}F_3N_3O_2$ (363.33): C, 59.50; H, 4.44; N, 11.57.Found: C, 59.40; H, 4.24; N, 11.37.IR (υ_{max}, cm^{-1}): 3464 (N-H), 3055 (Ar. C–H), 2949 (C–H aliphatic), 1509 (C=N), 1484 (Ar. C=C), 1177 (C–N), 1093 (C-O), 1085 (C-F).^{1}H NMR (400 MHz, $CDCl_3$); δ: 7.55 (d, *J* = 7.3 Hz, 2H), 6.98 (d, *J* = 7.3 Hz, 2H), 6.58 (s, 2H), 6.53 (s, 1H), 5.72 (d, *J* = 7.3 Hz, 1H), 4.38 (d, *J* = 7.1 Hz, 1H), 3.81 (s, 3H), 2.91 (s, 3H), 1.93 (s, 1H).LCMS: Calculated for $C_{18}H_{16}F_3N_3O_2$ $[M+H]^+$363.33, found 363.37.

7-methoxy-2-(2-methoxyphenyl)-4-methyl-3,3a,4,8b-tetrahydroimidazo[4,5-b]indole (3k). Melting Point: 200-204ºC.Yield: 83 %.R_f value: 0.72.Solvent system: Benzene: Methanol (9.7: 0.3). Anal. Calcd. for $C_{18}H_{19}N_3O_2$ (309.36): C, 69.88; H, 6.19; N, 13.58.Found: C, 69.78; H, 6.09; N, 13.38.IR (υ_{max}, cm^{-1}): 3414 (N-H), 3068 (Ar. C–H), 2917 (C–H aliphatic), 1576 (C=N), 1435 (Ar. C=C), 1143 (C–N), 1065 (C-O).^{1}H NMR (400 MHz, $CDCl_3$); δ: 7.58 (dd, *J* = 1.3 Hz, 1H), 7.31 – 7.27 (m, 1H), 6.99 – 6.91 (m, 2H), 6.57 (s, 2H), 6.53 (s, 1H), 5.39 (d, *J* = 7.3 Hz, 1H), 4.38 (d, *J* = 7.1 Hz, 1H), 3.83 – 3.81 (m, 6H), 2.94 (s, 3H), 2.51 (s, 1H).LCMS: Calculated for $C_{18}H_{19}N_3O_2$ $[M+H]^+$309.36, found 309.39.

7-methoxy-2-(4-methoxyphenyl)-4-methyl-3,3a,4,8b-tetrahydroimidazo[4,5-b]indole (3l). Melting Point: 208-212ºC.Yield: 77 %.R_f value: 0.64.Solvent system: Benzene: Methanol (9.7: 0.3). Anal. Calcd. for $C_{18}H_{19}N_3O_2$ (309.36): C, 69.88; H, 6.19; N, 13.58.Found: C, 69.78; H, 6.09; N, 13.38.IR (υ_{max}, cm^{-1}): 3452 (N-H), 3041 (Ar. C–H), 2971 (C–H aliphatic), 1518 (C=N), 1431 (Ar. C=C), 1174 (C–N), 1095 (C-O).^{1}H NMR (400 MHz, $CDCl_3$); δ: 7.56 (d, *J* = 7.1 Hz, 2H), 6.94 (d, *J* = 7.3 Hz, 2H), 6.65 – 6.60 (m, 2H), 6.56 (d, *J* = 6.9 Hz, 1H), 5.41 (d, *J* = 7.3 Hz, 1H), 4.38 (d, *J* = 7.1 Hz, 1H), 3.82 – 3.80 (m, 6H), 2.92 (s, 3H), 2.13 (s, 1H). LCMS: Calculated for $C_{18}H_{19}N_3O_2$ $[M+H]^+$309.36, found 309.32.

7-methoxy-4-methyl-2-phenyl-3,3a,4,8b-tetrahydroimidazo[4,5-b]indole (3m). Melting Point: 210-214ºC.Yield: 85 %.R_f value: 0.76.Solvent system: Benzene: Methanol (9.7: 0.3). Anal. Calcd. for $C_{17}H_{17}N_3O$ (279.34): C, 73.10; H, 6.13; N, 15.04.Found: C, 53.10; H, 6.03; N, 15.04.IR (υ_{max}, cm^{-1}): 3451 (N-H), 3086 (Ar. C–H), 2908 (C–H aliphatic), 1545 (C=N), 1487 (Ar. C=C), 1161 (C–N), 1087 (C-O).^{1}H NMR (400 MHz, $CDCl_3$); δ: 7.56 – 7.53 (m, 2H), 7.33 – 7.30 (m, 3H), 6.57 (s, 2H), 6.53 (s, 1H), 5.72 (d, *J* = 7.3 Hz, 1H), 4.38 (d, *J* = 7.1 Hz, 1H), 3.81 (s, 3H), 2.91 (s, 3H), 1.96 (s, 1H). LCMS: Calculated for $C_{17}H_{17}N_3O$ $[M+H]^+$279.34, found 279.38.

2-(4-isopropylphenyl)-7-methoxy-4-methyl-3,3a,4,8b-tetrahydroimidazo[4,5-b]indole (3n). Melting Point: 224-228ºC. Yield: 87 %.R_f value: 0.59. Solvent system: Benzene: Methanol (9.7: 0.3). Anal. Calcd. for $C_{20}H_{23}N_3O$ (321.42): C, 74.74; H, 7.21; N, 13.07. Found: C, 74.54; H, 7.11; N, 13.07. IR (υ_{max}, cm^{-1}): 3478 (N-H), 3065 (Ar. C–H), 2941 (C–H aliphatic), 1565 (C=N), 1432 (Ar. C=C), 1187 (C–N), 1095 (C-O).^{1}H NMR (400 MHz, $CDCl_3$); δ: 7.56 (d, *J* = 7.1 Hz, 2H), 7.32 (d, *J* = 7.3 Hz, 2H), 6.60 – 6.53 (m, 3H), 5.51 (d, *J* = 7.3 Hz, 1H), 4.38 (d, *J* = 7.1 Hz, 1H), 3.83 (s, 3H), 3.11 – 3.02 (m, 1H), 2.91 (s, 3H), 1.96 (s, 1H), 1.33 – 1.32 (m, 6H).LCMS: Calculated for $C_{20}H_{23}N_3O$ $[M+H]^+$321.42, found 321.47.

2-(4-(tert-butyl)phenyl)-7-methoxy-4-methyl-3,3a,4,8b-tetrahydroimidazo[4,5-b]indole (3o). Melting Point: 220-224ºC.Yield: 83 %.R_f value: 0.75.Solvent system: Benzene: Methanol (9.7: 0.3). Anal. Calcd. for $C_{21}H_{25}N_3O$ (335.44): C, 75.19; H, 7.51; N, 12.53. Found: C, 75.09; H, 7.31; N, 12.43.IR (υ_{max}, cm^{-1}): 3478 (N-H), 3032 (Ar. C–H), 2946 (C–H aliphatic), 1517 (C=N), 1474 (Ar. C=C), 1163 (C–N), 1042 (C-O).^{1}H NMR (400 MHz, $CDCl_3$); δ: 7.52 (d, *J* = 7.1 Hz, 2H), 7.33 (d, *J* = 7.3 Hz, 2H), 6.65 – 6.56 (m, 3H), 5.41 (d, *J* = 7.3 Hz, 1H), 4.38 (d, *J* = 7.1 Hz, 1H), 3.81 (s, 3H), 2.92 (s, 3H), 2.11 (s, 1H), 1.37 (s, 9H).LCMS: Calculated for $C_{21}H_{25}N_3O$ $[M+H]^+$335.44, found 335.48.

***In vitro* Antimicrobial Activity.** The synthesized compounds (**3a-3o**) were screened for antimicrobial activity and the cup plate method was used for the determination zone of inhibition.Two gram-positive bacterial strains *Staphylococcus aureus, Bacillus anthracis, and* two gram-negative bacterial strains *Pseudomonas aeruginosa and Escherichia coli* were used for the determination of antibacterial activity. Two fungal strains *C. albicans* and *A. niger* were used for the determination of antifungal activity. Streptomycin and Fluconazole were utilized as a benchmark for assessing antibacterial and antifungal properties, respectively. The solvent employed was dimethyl sulfoxide (DMSO). The Culture Media utilized for bacteria and fungi were Nutrient broth and Sabourd dextrose broth, respectively. Sterile nutrition broth and sabourd dextrose broth plates were made by aseptically pouring sterile agar into Petri dishes. 0.1 ml of each standardized test organism was evenly distributed onto agar plates. Preparation of holes was conducted using a sterile borer with a diameter of 6 mm. The experimental medication, together with the reference drug and the control solvent, were individually inserted in each respective hole. Subsequently, the plates were kept at a temperature of 4°C for 1 hour to facilitate the dispersion of the solution into the medium. The bacterial plates were subjected to incubation at a temperature of 37°C for 24 hours, while the fungal plates were incubated at a temperature of 25°C for 48

hours. The diameter of the zone of inhibition was measured in millimeters (Bowen, 2017; Singaravelu *et al*., 2019; Singaravelu *et al*., 2017; Hegaziand Abd Allah 2012; Risan *et al*., 2017).

***In silico* Study**

***In-silico* prediction of absorption and drug-likeness.** The molecular properties ofthe listed compounds were analyzed by usingthe SwissADME online server to validate them as potential ligands against therapeutic targets.

Lipinski rule or rule of five is like that to be drug-like, a candidate should have less than five hydrogen bond donors (HBD), less than 10 hydrogen bond acceptors (HBA), a molecular weight of less than 500 Da, and a partition coefficient log P of less than 5. The rule of five aims to highlight possible bioavailability problems if two or more properties are violated (Ranjith and Ravikumar 2019; Tripathi *et al*., 2019; Riyadi, 2021; Ilieva *et al*., 2018).

"Absorption (%ABS) was calculated by %ABS = 109-(0.345 X TPSA)"(Ariffin *et al*., 2014; Maximo da Silva*et al*., 2015; Ren *et al*., 2021).

Molecular Docking Studies. Windows 10 (64-bit) operating systems with 4 GB RAM and 2.50 GHz Intel(R) Core(TM) i5-7200U processor were used for executing the docking process. PyRx version 0.8, available at https://pyrx.sourceforge.io/ was used to perform the docking in Auto Dock Vina Wizard. Autodock Tools 4.2.6 which is made accessible by the Scripps Research Institute at https://autodock.scripps.edu/, was used for preparing the proteins and for grid generation, Ligands were processed using Open babeland PyRx 0.8 and interaction poses of ligands were visualized and analyzed using Discovery Studio Visualizer. The proteins were prepared using Autodock vina. In this step, attached water molecules and bound heteroatoms/ligands were removed, polar hydrogens and Kollman charges were added, the charge was spread equally over all atoms, and residues were checked for missing atoms if any. The prepared PDB files were then converted to the PDBQT format for executing the next step. Ligands in smiles format were converted to SDF file format and 3D coordinates for all ligands were generated using Open Babel using the command line. The 3D structure data files were processed in PyRx using UFF energy minimization and then converted to PDBQT format (autodock detectable format).The grid box was first set over attached ligands using AutoDock Tools and then manually adjusted to the desired dimensions in PyRx. The grid dimensions were set as 30.329 × 40.334 × 80.415 A^{o3} keeping several points as 25 in X, Y, and Z directions for PDB ID:2EG7 and -7.362 × 5.378 × 1.119 A^{o3} keeping some points as 20 in X, Y, Z direction for PDB ID:5D6P.The docking was implemented in Vina Wizard of PyRx Tool, using exhaustiveness of 8, and the resultant out files were split into individual pose files. These files and the protein structure were then taken for visualization of interactions using Maestro Visualizer (Kondapuram *et al*., 2021; Muhammad and Fatima, 2015, Herowati and Widodo, 2014; Soudani *et al*., 2021).

RESULT AND DISCUSSION

Chemistry

General Procedure for Synthesis of imidazo[4,5-b]indole derivatives 3(a-o). A 500 mL round-bottom flask fitted with a reflux condenser and taken stirring solution of compound 1 (2.62 mmol) neat, was taken at 25°C with maintaining nitrogen atmosphere and stirred the reaction mixture vigorously and added different substituted compound 2 (3.14 mmol), Silica Sulfuric Acid (0.05 mmol) as a catalyst at110 °C for 4 h reflux. The reaction was then brought to room temperature. The reaction was monitored by checking TLC. After completion of the reaction, the reaction mixture was quenched with water (20 mL) extracted with EtOAc (25 × 3 mL), the combined organic layer was washed with water and brine, dried over the anhydrous Na_2SO_4, and concentrated under reduced pressure, to afford compounds 3(a-o) (80-150 mg, 20-35%).

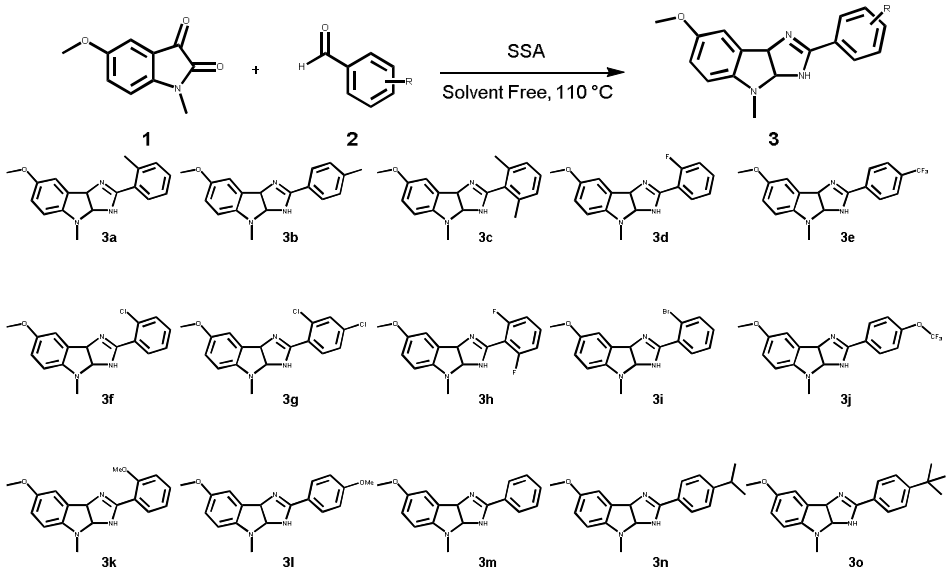

***In vitro* Antimicrobial Activity.** The synthesized title compounds (3a-3o) were evaluated for their antimicrobial activity against two gram-positive bacterial strains, *Staphylococcus aureus and Bacillus anthracis,* as well as two gram-negative bacterial strains, *Pseudomonas aeruginosa, and Escherichia coli*. Additionally, two fungal strains, *C. albicans* and *A. niger*, were also tested. The cup-plate method was used for the antimicrobial activity assessment. Compounds **3e** and **3i** had the highest level of effectiveness against all the strains. When comparing the streptomycin and fluconazole compounds, it is observed that **6e** has significant and potent outcomes.

Table 1: Antimicrobial Activity of Title compounds (3a-3o).

Compound (1000 µg/ml)	Zone of Inhibition (mm)					
	S. aureus	*B. anthracis*	*P. aeruginosa*	*E. coli*	*C. albicans*	*A. niger*
Streptomycin	**36**	**35**	**32**	**33**	**-**	**-**
Fluconazole	**-**	**-**	**-**	**-**	**29**	**31**
3a	21	19	14	15	11	11
3b	25	17	10	17	14	17
3c	23	15	13	10	16	17
3d	20	14	14	20	17	18
3e	25	27	24	27	21	23
3f	16	7	21	18	19	18
3g	23	19	11	24	17	16
3h	11	9	13	16	12	11
3i	28	28	25	24	23	25
3j	25	18	10	17	14	13
3k	29	25	26	25	21	18
3l	17	9	19	21	13	14
3m	23	18	19	19	14	16
3n	15	20	15	11	13	12
3o	30	26	26	24	20	17

Molecular Docking Studies

Table 2: Molecular Docking of Compounds (3a-3o) against PDB id: 2EG7.

Compounds	Binding Affinity	H-bond	Hydrophobic bonding
3a	-7.8	ARG20	TYR79, PRO105, TYR104, THR143, KCX102, LEU222, HIS177, HIS16, HIS18, ALA252, HIS254
3b	-7.5	ARG20	ASN44, PRO105, THR143, KCX102, TYR104, HIS177, HIS139, HIS18, ARG20, ALA252, HIS254
3c	**-8.1**	ARG20	ASN44, PRO105, THR143, KCX102, TYR104, HIS177, HIS139,TYR79, HIS16, HIS18, ARG20, ALA252, HIS254, LEU222
3d	-7.9	ARG20	HIS139, TYR79, KCX102, TYR104,PRO105,THR143,ARG20, ASN44, HIS18, HIS16, HIS254, ALA252
3e	-7.7	-	HIS139, TYR104, PRO105,ANS107, THR110, THR143, TYR79, ANS44, ASP250, ALA252, HIS254, ARG20, GLY267, ALA266
3f	-7.9	ARG20	HIS 177, LEU222, KCX102, HIS139, TYR104, PRO105, THR143, TYR79, ASN44, HIS 18, HIS18, HIS 254, ALA252
3g	-7.8	ARG20	THR143, PRO 105, TYR104, KCX 102, TYR79, HIS139, HIS177, ALA252, HIS254, HIS16, HIS18, ANS44, ARG2O
3h	-8	ARG20	HIS139, TYR79, KCX102, TYR104, PRO105, THR143, ARG20, ASN44, HIS18, HIS16, HIS 254, ALA252
3i	-7.7	ARG20	HIS177, ASP 250, LEU 222, HIS139, ASN44, TYR79, TYR 104, PRO 105, ARG20, HIS254, HIS18
3j	-7.8	-	PRO105, TYR104, KCX102, HIS177, HIS139 HIS18, ARG2O, ALA252, HIS254, ANS44, HIS144, GLY155, VAL166, THR11O, TYR79
3k	-7.4	ARG20	THR143, LEU222, HIS139, HIS177, ASP250, ASN44, HIS18, HIS254, ARG2O, TYR79, TYR104,PRO105
3l	-7.5	LEU222	HIS139, HIS254, ALA252, ASP250, ALA266, GLY267, CYS268, CYS221, ARG20, ASN44, TYR104, PRO105, ASN107, THR143
3m	-7.6	ARG20	ASN44, HIS18, HIS16, HIS 254, ALA252, HIS 177, HIS139, KCX102, TYR79, TYR104, PRO105, THR143
3n	-7.6	ARG20	ASN44, HIS 254, ALA252, ALA266, LEU 222, ANS107, HIS 177, HIS139, KCX102, TYR79, TYR104, PRO105, THR143
3o	-7.6	-	ALA266, LEU 222, GLY267, HIS 254, ALA252, ASP 250, ARG20, HIS18, TYR79, TYR104, PRO105, ASN107 ARG152, THR 143
Ciprofloxacin	-7.7	KCX 102	HIS 139, PRO 105, TYR 104, LEU 222, HIS 16, HIS 18, ARG 20, ASP 250, ALA 252, HIS 254, HIS 177
Fluconazole	-6.8	-	HIS 254, ALA 252, ASP 250, PRO 105, TYR 104, KCX 102, HIS 139, LEU 22, HIS 177, HIS 16, ALA 266, HIS 18, ARG 20
Streptomycin	-8.3	ANS 44, ALA 266, HIS 177	HIS 114, PRO 48, TYR 79, ALA 46, LEU 45, ARG 258, GLY 256, ALA 266, HIS 254, ALA 252, ASP 250, ARG 20, HIS 18, HIS 16, KCX 102 LEU 222, TYR 104, PRO 105, HIS 139

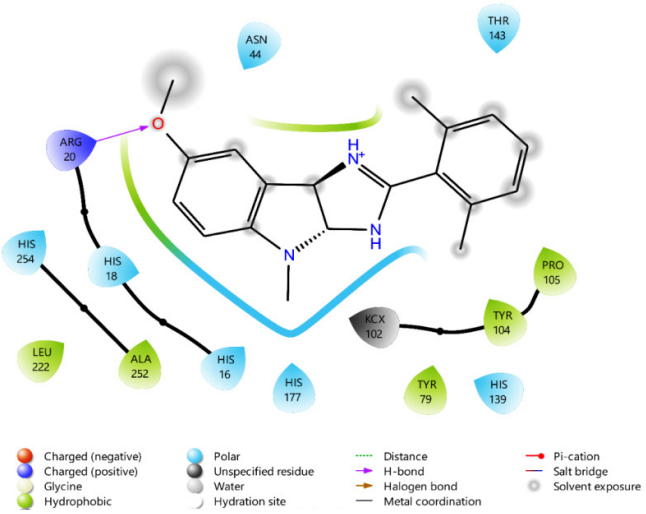

Fig. 1. Binding Pattern of **3c** against PDB id: 2EG7.

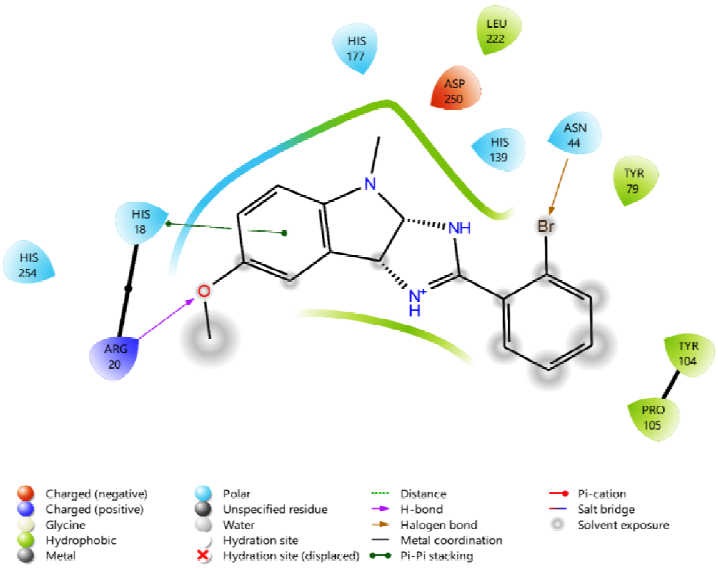

Fig. 2. Binding Pattern of **3h** against PDB id: 2EG7.

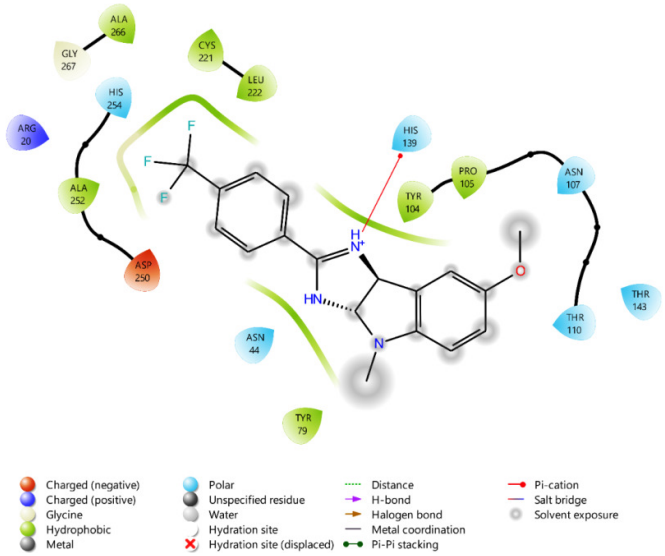

Fig. 3. Binding Pattern of **3e** against PDB id: 5D6P.

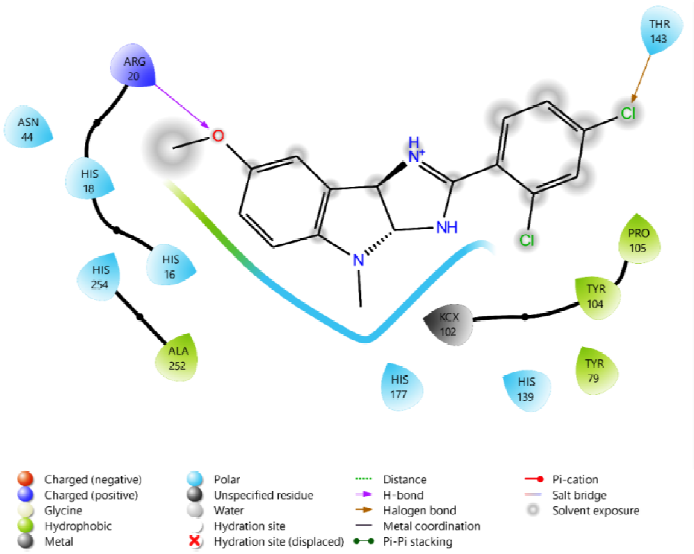

Fig. 4. Binding Pattern of **3g** against PDB id: 5D6P.

Table 3: Molecular Docking of Compounds (3a-3o) against PDB id: 5D6P.

Compounds	Binding Affinity	H-bond	Hydrophobic bonding
3a	-7.9	-	VAL 79, ASP 81, ARG 84, ILE 86, ILE 102, GLU 58, ASP 57, SER 55, ASN 54, ILE 51
3b	-8	-	SER 129, ILE 102, LEU 103, ILE 51, THR 173, ILE 175, ILE 51, ASN 54, SER 55, GLU 58, ASP 81, ARG 84, GLY 85, ILE 86, PRO 87, ARG 144
3c	-7.9	-	GLU 58, ASP 57, SER 55, ASN 54, ILE 51, THR 173, ILE 175, VAL 79, ASP 81, ILE 102, ARG 84, ILE 86, PRO 87,
3d	-7.9	-	ILE 86, GLU 58, ARG 84, ASP 57, ARG 84, SER 55, ASN 54, ASP 81, VAL 49, ILE 51, THR 173, ILE 175, IL;E 102
3e	**-8.2**	-	ILE 175, THR 173, ILE 51, ASN 54, SER 55, GLU 58, VAL 79, ASP 81, ARG 84 GLY 85, ILE 86, PRO 84, ARG 144, ILE 102
3f	-7.9	-	THR 173, ILE 175, ILE 51, ASN 54, SER 55, ASP 57, GLU 58, VAL 79, ASP 81, ARG 84, ILE 86, ILE 102
3g	**-8.1**	-	ILE 102, VAL 49, ILE 51, ASP 81, THR 173, ASN 54, ARG 84, ILE 175, SER 55, ILE 86, ASP 57, GLU 58, ALA 61
3h	-8.1	-	ILE 175, THR 173, ILE 51, ASN 54, SER 55, GLU 58, ASP 81, ARG 84, GLY 85, ILE 86, SER 129, ILE 102 LEU 103
3i	-7.3	-	ASP 81, THR 173, ILE 175, GLU 58, ASP 57, SER 55, ASN 54, ILE 51, ILE 102, ILE 86, PRO 87
3j	-7.9	ARG 144	PRO 87, ILE 86, GLY 85, ARG 84, ASP 81, ILE 51, THR 173, ASN 54, SER, 55, GLU 58
3k	-7.1	-	VAL 79, ASP 81, ILE 51, ILE 86, ASN 54, SER, 55, ASP 57, GLU 58, ILE 102, ILE 175, THR 173
3l	-8	-	ARG 144, SER 129, ILE 51, LEU 103, ASN 54, SER 55, ILE 175, THR 173, GLU 58, ASP 81, ARG 84, GLY 85, ILE 86, PRO 87
3m	-7.9	-	ILE 102, VAL 79, ASP 81, ARG 84, GLY 85, ILE 86, PRO 87, ILE 51, ASN 54, SER 55, GLU 58, ILE 175, THR 173, ARG 144
3n	-7.8	-	ILE 102, VAL 79, ASP 81, ARG 84, GLY 85, ILE 86, PRO 87, ILE 51, ASN 54, SER 55, GLU 58, ILE 175, THR 173, ARG 144
3o	-7.8	THR 173, ASN 54	ILE 86, GLY 85, ARG 84, ASP 81, GLU 58, GLU 50, TYR 35, VAL 130, SER 129, SER 128, VAL 101, ILE 102, LEU 103
Ciprofloxacin	-8.3	ASN 54, GLY 85	ILE 102, PRO 87, ILE 86, ARG 84, GLY 83, ASP 81, ILE 175, THR 173
Fluconazole	-7.2	ANS 54,	LEU 103, ILE 51, ASP 57, GLU 58, ASP 81, GLY 83, ARG 84, GLY 85, ILE 86, ILE 175, THR 173
Streptomycin	-7.2	ASP 81	ASN 54, SER 55, ASP 57, GLU 58, ALA 61, PRO 87, ILE 86, GLY 85, ARG 84, GLY 83, THR 173, ASP 81, ILE 102

The docking studies of novel compounds were performed at different binding sites like PDB ID 2EG7-*E. coli* Dihydrorootase in complex with HDDP and PDB ID 5D6P-ATP Binding domain of GyrB of *S. aureus* in complex with 57U were chosen. Table 2 and Fig. 1 to 4 illustrate the docked conformations and docking results of ligands in the active site. According to these findings, the targeted molecules established a large number of hydrogen bonds, engaged in charged and hydrophobic interactions, π-cation, and π-π

stacking, and showed significant and varied binding affinities towards all binding sites. The majority of the compounds exhibited interactions through hydrogen bonds with various amino acid residues at various binding sites. The best binding interaction with the highest binding affinity according *in silico* and *in vitro* studies is **3c** and **3h** for **2EG7** in the comparison study with Ciprofloxacin, Fluconazole, and Streptomycin. We observe top selected ligands involved in H-bond, π-cation, charged, hydrophobic, and π-stacking interactions and additional contacts at the binding site. Compound **3c** showed different interactions with ASN44, PRO105, THR143, KCX102, TYR104, HIS177, HIS139, TYR79, HIS16, HIS18, ARG20, ALA252, HIS254, and LEU222 and compound **3h** showed different interactions with HIS139, TYR79, KCX102, TYR104, PRO105, THR143, ARG20, ASN44, HIS18, HIS16, HIS 254, and ALA252 with a binding energy of -8.1, -8.0. For another interaction site **5D6P** the compound **3e, 3h** is the most promising agents in the comparison of Ciprofloxacin, Fluconazole, and Streptomycin. Compound **3e** showed different interactions with ILE175, THR173, ILE51, ASN54, SER55, GLU58, VAL79, ASP81, ARG84 GLY85, ILE86, PRO84, ARG144, and ILE102 and compound **3h** showed different interactions with ILE175, THR173, ILE51, ASN54, SER55, GLU58, ASP81, ARG84, GLY85, ILE86, SER129, ILE102, and LEU103 with a binding energy of -8.2, -8.1. According to *in vitro* Antimicrobial Activity the compound **3i**, and **3k** are the most promising agents.

ADMET Studies

Table 4: In silico Drug Likeness and absorption.

Comp	Molecularweight	Num. rotatablebonds	Num. H-bondacceptors	Num.H-bonddonors	TPSA(Å²)	Log Po/w (iLOGP)	GI Absorption	Lipinski	Predicted%Absorption
3a	293.36	2	2	1	36.86	2.98	High	0	96.28
3b	293.36	2	2	1	36.86	3.07	High	0	96.28
3c	307.39	2	2	1	36.86	2.82	High	0	96.28
3d	297.33	2	3	1	36.86	2.45	High	0	96.28
3e	347.33	3	5	1	36.86	2.86	High	0	96.28
3f	313.78	2	2	1	36.86	2.61	High	0	96.28
3g	348.23	2	2	1	36.86	3.20	High	0	96.28
3h	315.32	2	4	1	36.86	2.71	High	0	96.28
3i	358.23	2	2	1	36.86	2.70	High	0	96.28
3j	363.33	4	6	2	46.09	3.07	High	0	93.10
3k	309.36	3	3	1	46.09	2.45	High	0	93.10
3l	309.36	3	3	1	46.09	3.05	High	0	93.10
3m	279.34	2	2	1	36.86	2.59	High	0	96.28
3n	321.42	3	2	1	36.86	3.24	High	0	96.28
3o	335.44	3	2	1	36.86	3.35	High	0	96.28

SUMMARY AND CONCLUSION

This study presents the synthesis, docking, ADMET, and antibacterial activity analysis of a new series of derivatives. All of the substances demonstrate strong antimalarial activity in laboratory tests, with some approaching the effectiveness of Ciprofloxacin, Fluconazole, and Streptomycin. The compounds with the given title were evaluated for their interaction with two distinct binding sites. Compounds **3c**, **3e**, and **3h** were identified as the most powerful compounds based on docking experiments. Compounds **3i** and **3k** are considered the most promising compounds according to the *in silico* and *in vitro* results. The two most potent compounds in the series were identified **3i**, and **3k** with respective values of *E. coli* Dihydroorootase complex and GyrB of *S. aureus*. This series of compounds offers lead-like compounds for research and demonstrates good binding affinity with different modeled proteins. As a result, the current work promotes the development of fresh antimicrobial agents by pharmacophore hybridization.

FUTURE SCOPE

The new findings might be useful for scientist in futureresearch and development of imidazo[4,5-b]indole nucleus as neweranti- microbial agents.

Acknowledgement. The authors deeply appreciate theassistance of the Department of Chemistry, Bhupal Nobles'University, Udaipur-313001, India

Conflict of Interest. None.

REFERENCES

Abushaheen, M. A., Fatani, A. J., Alosaimi, M., Mansy, W., George, M., Acharya, S., and Jhugroo, P. (2020). Antimicrobial resistance, mechanisms and its clinical significance. *Disease-a-Month*, *66*(6), 100971.

Ariffin, A., Rahman, N. A., Yehye, W. A., Alhadi, A. A., and Kadir, F. A. (2014). PASS-assisted design, synthesis and antioxidant evaluation of new butylated hydroxytoluene derivatives. *European Journal of Medicinal Chemistry*, *87*, 564-577.

Ballal, M. (2016). Trends in antimicrobial resistance among enteric pathogens: a global concern. *Antibiotic Resistance*, 63-92.

Barman, P., Ghosh, D. and Saha, A. (2023). Phytochemical and Antimicrobial Assessment of Leafy Vegetables Collected from Solid Waste Dumping Ground and

Normal Ground - A Comparative Study. *Biological Forum – An International Journal, 15*(3), 298-304.

Bowen, K. (2017). Protecting Regulatory Expressions of Food Populism through Interstate Cooperation. *Tenn. L. Rev.*, *85*, 1-71.

De Villiers, M. (2019). Attack of the Superbugs: The Law and Medicine of Antibiotic Resistance. *Alb. LJ Sci. and Tech.*, *29*, 270-314.

Djihane, B., Wafa, N., Elkhamssa, S., Maria, A. E., and Mihoub, Z. M. (2017). Chemical constituents of Helichrysum italicum (Roth) G. Don essential oil and their antimicrobial activity against Gram-positive and Gram-negative bacteria, filamentous fungi and Candida albicans. *Saudi Pharmaceutical Journal*, *25*(5), 780-787.

Duvvi, N. B., Suneetha, N. N., Kumar, N. A., Nagadesi, P. K. and Yenumula, V. N. D. R. (2019). Mycogenic synthesis of copper nano-particles by Bio-controlling fungi (Aspergillus niger and Trichoderma viride) and its Antifungal activity on Plant Pathogens. *International Journal on Emerging Technologies, 10(*4), 10–16.

Ferri, M., Ranucci, E., Romagnoli, P., and Giaccone, V. (2017). Antimicrobial resistance: A global emerging threat to public health systems. *Critical reviews in food science and nutrition*, *57*(13), 2857-2876.

Hashiguchi, T. C. O., Ouakrim, D. A., Padget, M., Cassini, A., and Cecchini, M. (2019). Resistance proportions for eight priority antibiotic-bacterium combinations in OECD, EU/EEA and G20 countries 2000 to 2030: a modelling study. *Eurosurveillance*, *24*(20), 1800445.

Hegazi, A. G., and Abd Allah, F. M. (2012). Antimicrobial activity of different Saudi Arabia honeys. *Global Veterinaria*, *9*(1), 53-59.

Herowati, R., and Widodo, G. P. (2014). Molecular Docking studies of chemical constituents of Tinospora cordifolia on glycogen phosphorylase. *Procedia Chemistry*, *13*, 63-68.

Hillock, N. T., Merlin, T. L., Turnidge, J., and Karnon, J. (2022). Modelling the future clinical and economic burden of antimicrobial resistance: the feasibility and value of models to inform policy. *Applied Health Economics and Health Policy*, *20*(4), 479-486.

Ilieva, Y., Kokanova-Nedialkova, Z., Nedialkov, P., and Momekov, G. (2018). In silico ADME and drug-likeness evaluation of a series of cytotoxic polyprenylated acylphloroglucinols, isolated from Hypericum annulatum Morris subsp. annulatum. *Bulg. Chem. Commun*, *50*, 193-199.

Kaur, M., Singh, P., Kaur, G., Kaur, M., Sharma, J., Kumar, M., Sharma, M., and Kumar, A. (2019). Development of Colloidal Semiconductor Nanocrystals: Synthesis, Properties and their Outlook for Light Emitting Diodes (LEDs). *International Journal on Emerging Technologies, 10*(1), 16-34.

Kondapuram, S. K., Sarvagalla, S., and Coumar, M. S. (2021). Docking-based virtual screening using PyRx Tool: autophagy target Vps34 as a case study. In *Molecular Docking for Computer-Aided Drug Design* (pp. 463-477). Academic Press.

Kumar, G. and Nanda, S. (2021). Molecular Perspectives of Plant-Pathogen Interactions: An Overview on Plant Immunity. *Biological Forum – An International Journal, 13*(1), 48-53.

Makena, A., Düzgün, A. Ö., Brem, J., McDonough, M. A., Rydzik, A. M., Abboud, M. I., and Schofield, C. J. (2016). Comparison of Verona integron-borne metallo-β-lactamase (VIM) variants reveals differences in stability and inhibition profiles. *Antimicrobial agents and chemotherapy*, *60*(3), 1377-1384.

Malaviya, A., and Mishra, N. (2011). Antimicrobial activity of tropical fruits. *Biological Forum – An International Journal, 3*(1), 1-4.

Marshall, B., Broecker, K., McGowan, E., and Young, K. (2014). Tracking antibiotic resistance genes in the environment. *APUA Newsletter*, *32*(2), 19-20.

Marston, H. D., Dixon, D. M., Knisely, J. M., Palmore, T. N., and Fauci, A. S. (2016). Antimicrobial resistance. *Jama*, *316*(11), 1193-1204.

Maximo da Silva, M., Comin, M., Santos Duarte, T., Foglio, M. A., De Carvalho, J. E., do Carmo Vieira, M., and Nazari Formagio, A. S. (2015). Synthesis, antiproliferative activity and molecular properties predictions of galloyl derivatives. *Molecules*, *20*(4), 5360-5373.

Muhammad, S. A., and Fatima, N. (2015). In silico analysis and molecular docking studies of potential angiotensin-converting enzyme inhibitor using quercetin glycosides. *Pharmacognosy magazine*, *11*(Suppl 1), S123-S126.

Peyrani, P., Mandell, L., Torres, A., and Tillotson, G. S. (2019). The burden of community-acquired bacterial pneumonia in the era of antibiotic resistance. *Expert review of respiratory medicine*, *13*(2), 139-152.

Ranjith, D., and Ravikumar, C. (2019). SwissADME predictions of pharmacokinetics and drug-likeness properties of small molecules present in Ipomoea mauritiana Jacq. *Journal of Pharmacognosy and Phytochemistry*, *8*(5), 2063-2073.

Ren, B., Liu, R. C., Ji, K., Tang, J. J., and Gao, J. M. (2021). Design, synthesis and in vitro antitumor evaluation of novel pyrazole-benzimidazole derivatives. *Bioorganic and medicinal chemistry letters*, *43*, 128097.

Risan, M. H., Taemor, S. H., Muhsin, A. H., and Hussan, S. (2017). Antibacterial activity of Agaricus bisporus and Pleurotus ostreatus extracts against some gram negative and positive bacteria. *Eur. J. Biomed*, *4*, 9-15.

Riyadi, P. H., Sari, I. D., Kurniasih, R. A., Agustini, T. W., Swastawati, F., Herawati, V. E., and Tanod, W. A. (2021). SwissADME predictions of pharmacokinetics and drug-likeness properties of small molecules present in spirulina platensis. In *IOP conference series: earth and environmental science* (Vol. 890, No. 1, p. 012021). IOP Publishing.

Russo, A., Franchina, T., Ricciardi, G. R. R., Picone, A., Ferraro, G., Zanghì, M., and Adamo, V. (2015). A decade of EGFR inhibition in EGFR-mutated non small cell lung cancer (NSCLC): Old successes and future perspectives. *Oncotarget*, *6*(29), 26814.

Sharma, R.N. (2010). Synthesis, characterization, and biological activities of new 1-[(2,5-dichloroanilinomalonyl)-3-(N-2'-cyanoethyl)-2-(N-acetyl) 2,5-dichloroanilino)]-5-phenyl pyrazoline derivatives. *International Journal of Theoretical & Applied Sciences, 2*(1): 4-13

Singaravelu, S., Sankarapillai, J., Chandrakumari, A. S., and Sinha, P. (2019). Effect of Azadirachta indica crude bark extracts concentrations against gram-positive and gram-negative bacterial pathogens. *Journal of Pharmacy and Bioallied Sciences*, *11*(1), 33-37.

Soudani, W., Hadjadj-Aoul, F. Z., Bouachrine, M., and Zaki, H. (2021). Molecular docking of potential cytotoxic alkylating carmustine derivatives 2-chloroethylnitrososulfamides analogues of 2-chloroethylnitrosoureas. *Journal of Biomolecular Structure and Dynamics*, *39*(12), 4256-4269.

Torre, L. A., Bray, F., Siegel, R. L., Ferlay, J., Lortet-Tieulent, J., and Jemal, A. (2015). Global cancer statistics, 2012. *CA: a cancer journal for clinicians*, *65*(2), 87-108.

Tripathi, P., Ghosh, S., and Talapatra, S. N. (2019). Bioavailability prediction of phytochemicals present in *Calotropis procera* (Aiton) R. Br. by using Swiss-ADME tool. *World Scientific News*, (131), 147-163.

Waithaka, P. N., Gathuru, E. M., Githaiga, B. M., Ochieng, E. O., and Laban, L. T. (2017). Microbial Degradation of Polythene using Actinomycetes Isolated from Maize Rhizosphere, Forest and Waste Damping sites within Egerton University, Kenya. *International Journal on Emerging Technologies, 8*(1), 05-10.

Ziegler, M. (2014). The Black Death and the future of the Plague. *The Medieval Globe*, *1*(1), 11.

How to cite this article: Bhumika Ranawat, Renu Rathore, Ritu Tomar and Mangal Shree Dulawat (2023). Characterization and GC-MS Profiling of Volatile Compounds in an Anti-Ophidic Formulation from Haryana. *Biological Forum – An International Journal, 15*(5a): 757-766.